Advancing Near-Field Tsunami Fragility Modeling Through Structural Simulation and Post-Event Damage Observations

Mojtaba Harati * and John W. van de Lindt

Posted Date: 15 April 2026

doi: 10.20944/preprints202604.1022.v1

Keywords: near-field tsunami; fragility modeling; multi-hazard simulation; momentum flux; damage survey data

 doi:10.20944/preprints202604.1022.v1

Article

Advancing Near-Field Tsunami Fragility Modeling Through Structural Simulation and Post-Event Damage Observations

Mojtaba Harati and John W. van de Lindt *

Department of Civil and Environmental Engineering, Colorado State University, Fort Collins, CO, USA

* Correspondence: m.harati@colostate.edu

Abstract

Tsunami fragility modeling plays a central role in probabilistic coastal risk assessment; however, representing structural vulnerability under near-field tsunami conditions remains challenging due to complex hydrodynamic loading, strong spatial variability, and the presence of pre-existing earthquake damage. This paper provides a comprehensive review and synthesis of current approaches for modeling near-field tsunami impacts on infrastructure, with a particular focus on bridging simulation-based methods and empirical damage survey observations. The discussion highlights how successive hazard simulations can be used to capture coupled earthquake–tsunami effects, while damage surveys offer critical insights into observed relationships between structural damage, hydrodynamic intensity measures, and spatial characteristics such as coastal proximity. Special attention is given to the role of momentum flux as a physically meaningful predictor of damage and to the systematic differences between near-field and far-field fragilities. Building on these insights, the paper outlines practical strategies for adapting baseline fragility relationships to near-field conditions, including the use of spatially dependent intensity adjustments informed by empirical data. Rather than proposing a single methodology, this work aims to provide a structured perspective on existing knowledge and to guide researchers and practitioners in developing more physically consistent and data-informed fragility models for near-field tsunami risk and resilience assessments.

Keywords: near-field tsunami; fragility modeling; multi-hazard simulation; momentum flux; damage survey data

1. Introduction

Tsunamis are among the most devastating coastal hazards and have repeatedly demonstrated their impacts in causing catastrophic losses to coastal communities and infrastructure. Historical events such as the 2004 Indian Ocean tsunami and the 2011 Great East Japan tsunami revealed the enormous destructive potential of tsunami inundation and emphasized the need for systematic approaches to tsunami risk assessment and mitigation. Over the past two decades, the scientific community has made significant progress in developing quantitative frameworks for evaluating tsunami hazards and their potential impacts on the built environment [1–4]. In particular, probabilistic approaches to tsunami hazard and risk assessment have gained increasing attention as they allow for the explicit treatment of uncertainties associated with tsunami generation, propagation, and impact processes [5,6]. These developments are consistent with broader advances in probabilistic risk assessment methods that have long been applied in seismic hazard analysis and performance-based earthquake engineering [7–9]. More recently, probabilistic tsunami hazard and risk analysis frameworks have been widely adopted to support coastal disaster risk management and resilience planning initiatives [10,11].

 doi:10.20944/preprints202604.1022.v1

Tsunami risk assessment generally involves the integration of several interrelated components, including hazard characterization, exposure modeling, and vulnerability modeling. Within probabilistic tsunami hazard and risk frameworks, tsunami hazard is commonly described using intensity measures such as flow depth, flow velocity, run-up height, and momentum flux [12,13]. These intensity measures are typically obtained through numerical simulations that model tsunami generation, propagation across ocean basins, and subsequent inundation of coastal areas [6,11]. Compared with other natural hazards such as earthquakes, tsunami hazard assessment relies heavily on numerical simulations due to the limited availability of observational data and the strong influence of coastal bathymetry and topography on wave transformation and inundation patterns [5,10]. As emphasized in recent studies, modern tsunami hazard assessment workflows often involve simulation-based probabilistic frameworks that propagate uncertainties from the initial tsunami source characterization through hydrodynamic modeling and ultimately to impact estimation [11,14,15].

A critical component of tsunami risk assessment is vulnerability modeling, which establishes the relationship between tsunami hazard intensity measures and the expected consequences for exposed assets. In probabilistic tsunami risk frameworks, vulnerability is commonly represented through fragility relationships that quantify the probability of exceeding specified structural damage states as a function of tsunami intensity measures [16,17]. Fragility functions provide an essential link between the physical characteristics of tsunami waves and the resulting damage to buildings and infrastructure, allowing hazard information to be translated into estimates of structural damage, economic loss, or casualties [6,11]. In addition, vulnerability assessment is closely connected to broader concepts of risk governance and disaster risk reduction, as fragility models are frequently used to predicts potential damage and thus inform land-use planning, building code development, evacuation planning, and other risk mitigation strategies for coastal communities [18,19].

Several methodological approaches have been proposed for developing tsunami fragility relationships. Empirical approaches derive fragility functions directly from post-event damage observations collected during field surveys following major tsunami events [20,21]. Analytical approaches, in contrast, use structural analysis and hydrodynamic loading models to estimate structural response under tsunami forces [1,22]. Indicator-based approaches take a broader perspective by evaluating vulnerability through composite indicators that capture multiple dimensions of risk, including physical, economic, and social vulnerability [23]. Previous research has shown that tsunami damage is strongly influenced by hydrodynamic parameters such as flow depth, velocity, and momentum flux, highlighting the importance of accurately characterizing tsunami intensity measures when developing fragility models [6,10,24]. In practice, the choice of vulnerability modeling approach often depends on the availability of damage data, structural information, and computational resources available for the analysis [11].

Despite the considerable progress achieved in tsunami vulnerability assessment, several important challenges remain. Empirical fragility models are often limited by the scarcity and spatial variability of high-quality damage datasets, as well as uncertainties in estimating the local tsunami intensity measures at survey locations [24,25]. Analytical fragility models, on the other hand, require detailed structural modeling and accurate representation of complex tsunami loading mechanisms, which may introduce additional uncertainties if structural properties or loading conditions are poorly constrained [26]. Furthermore, the stochastic nature of tsunami hazards and the complex interactions between tsunami waves and coastal infrastructure make it difficult to capture the full range of possible damage scenarios using a single modeling approach [5,6]. These challenges have motivated increasing interest in hybrid approaches that combine physics-based simulations with empirical damage observations in order to improve fragility model calibration and reduce epistemic uncertainty in tsunami vulnerability assessments [11].

In this paper, we review the development of tsunami fragility relationships through the observations gained from simulation-based structural analysis and field survey damage data. The main purpose is to leverage both physics-based modeling and empirical observations to improve the

 doi:10.20944/preprints202604.1022.v1

reliability of tsunami fragility models for coastal structures. Particular emphasis is placed on near-field tsunami environments (see next section for more details), where waves generated by nearby seismic sources can reach coastal communities within minutes and produce highly variable hydrodynamic conditions. By combining simulation-based modeling with insights derived from post-tsunami damage surveys, this study seeks to provide improved understanding of tsunami-induced structural damage mechanisms and to contribute to more robust fragility modeling approaches for tsunami risk assessment.

2. Near-Field and Far-Field Tsunami Characteristics

Tsunamis are commonly classified into near-field and far-field events depending on the distance between the tsunami source and the impacted coastline and the corresponding travel time of the tsunami waves [27,28]. Near-field tsunamis occur when coastal regions are located close to the source of tsunami generation, typically associated with subduction zone earthquakes or submarine mass failures occurring near the coastline. In these cases, tsunami waves may reach coastal areas within minutes to tens of minutes after the triggering event [29]. In contrast, far-field tsunamis originate from distant sources and travel across ocean basins before reaching remote coastlines, often requiring several hours to arrive [13]. This classification is important because it directly influences warning times, hazard characteristics, and the spatial variability of tsunami inundation processes [5,10]. Near-field tsunami events, such as those observed during the 2011 Great East Japan earthquake, often produce the most severe impacts due to the limited time available for evacuation and the extreme hydrodynamic conditions that can develop near the source region [6,11].

The generation mechanisms and wave propagation characteristics of near-field and far-field tsunamis differ substantially due to variations in the physical processes controlling tsunami initiation and ocean-scale propagation. Most destructive tsunamis are generated by large subduction zone earthquakes that produce vertical displacement of the seafloor, resulting in the displacement of a large volume of water and the formation of long-wavelength tsunami waves [5,30]. However, tsunamis may also be generated by other mechanisms including submarine landslides, volcanic eruptions, and atmospheric disturbances. These different sources lead to distinct wave characteristics and spatial distributions of tsunami intensity [31,32]. In near-field settings, tsunami waves often retain stronger nonlinear characteristics and may exhibit highly variable wave heights and inundation patterns due to complex coastal bathymetry and local topographic effects [33]. In contrast, far-field tsunamis propagate across ocean basins as long waves whose characteristics are strongly influenced by basin geometry and wave dispersion effects before interacting with coastal environments [34,35].

The hydrodynamic characteristics of tsunami inundation play a critical role in determining structural damage and therefore must be carefully considered in fragility modeling. Key tsunami intensity measures commonly used in hazard and vulnerability analyses include flow depth, flow velocity, run-up height, and momentum flux, all of which influence the hydrodynamic forces acting on coastal structures [36]. High flow depths can generate large hydrostatic forces on building components, while high flow velocities contribute to significant hydrodynamic forces that may lead to structural failure or scour [37]. In addition, tsunami flows frequently transport debris such as vehicles, building fragments, and vegetation, which can generate impact forces that significantly amplify structural damage. Observations from major tsunami events have demonstrated that debris impact and debris accumulation can play a major role in building damage and infrastructure failure during tsunami inundation [38,39]. As a result, accurate representation of these hydrodynamic parameters is essential for developing realistic fragility relationships for tsunami-induced structural damage.

These physical characteristics have important implications for fragility modeling, particularly when distinguishing between near-field and far-field tsunami impacts. Fragility relationships aim to quantify the probability that a structure will reach or exceed a specified damage state given a particular hazard intensity measure [40]. However, the variability of tsunami loading conditions can

 doi:10.20944/preprints202604.1022.v1

introduce significant uncertainty in fragility estimation. Near-field tsunamis often involve complex hydrodynamic conditions with rapid changes in flow depth and velocity, leading to highly variable damage patterns even within relatively small geographic areas [31,41]. Such variability complicates the development of consistent empirical fragility relationships derived from post-event damage surveys. Consequently, simulation-based approaches that combine hydrodynamic modeling with structural analysis have become increasingly important tools for improving fragility estimation in tsunami risk assessments [42,43].

In addition to hydrodynamic effects, near-field tsunami events frequently occur very close in time with strong ground shaking generated by the causative earthquake, which can significantly influence the observed structural damage patterns. Buildings located in near-field tsunami zones may already experience varying degrees of structural damage due to seismic shaking before being subjected to tsunami inundation [44–46]. This rapid sequential loading condition introduces additional complexity in fragility modeling because the structural capacity of buildings may be reduced prior to the arrival of tsunami waves. Consequently, damage observed after near-field tsunami events may reflect the combined effects of earthquake-induced damage and tsunami loading [47–49]. This phenomenon highlights the importance of considering multi-hazard interactions in tsunami vulnerability assessments and fragility modeling, particularly in regions exposed to large subduction earthquakes where earthquake and tsunami hazards occur in rapid succession [50].

By accounting for differences in tsunami generation mechanisms, wave propagation behavior, hydrodynamic loading conditions, and multi-hazard interactions, fragility models can better represent the physical processes that govern tsunami-induced structural damage [51]. Such improvements are particularly important for developing reliable vulnerability models that can support coastal risk mitigation strategies and resilience planning in tsunami-prone regions.

3. Simulation-Based Tsunami Fragility Modeling for Near-Field Tsunamis

Simulation-based fragility modeling provides a systematic framework for evaluating the probability of structural damage under coupled earthquake–tsunami hazard scenarios [1,47,49,52,53]. In the context of near-field tsunami events, this approach becomes particularly important because structures may already experience significant damage from the preceding earthquake before the arrival of the tsunami wave [22,54]. Consequently, the fragility of structures exposed to tsunami loads cannot be assumed to be independent of the earthquake damage state. Traditional approaches may appear, at first glance, to allow estimation of conditional failure probabilities through Bayes-type formulations—$P(TS/EQ) = [P(EQ/TS)\ P(TS)]/P(EQ)$—that combine earthquake and tsunami fragility curves. However, terms such as $P(\mathrm{EQ} \mid \mathrm{TS})$ are not practically estimable, as they imply a conditional dependence that is not physically or statistically observable in realistic earthquake–tsunami sequences [55]. Consequently, rather than pursuing such formulations, conventional methodologies rely on simplified statistical relationships—often linear or empirically calibrated mappings—such as those adopted in FEMA (2019) [56], to approximate multi-hazard interactions in a tractable manner.

To address this difficulty, recent efforts have increasingly turned to direct numerical simulation frameworks in which conditional probabilities $P(TS \mid EQ)$ are obtained explicitly from large-scale successive vulnerability simulations, rather than through indirect probabilistic inference [1,22,52,54]. Among the most notable advances in this line of research are studies that derive fragility relationships directly from simulated structural responses under combined hazard loading scenarios — an approach that has gained particular traction in near-field tsunami modeling, where the coupling between ground shaking and inundation demands cannot be decoupled without significant loss of accuracy. While the broader literature on this topic is extensive, the discussion that follows focuses on the most recent and methodologically consequential contributions that have shaped how near-field tsunami structural response is currently understood and simulated.

 doi:10.20944/preprints202604.1022.v1

3.1. Near-Field Tsunami Fragility Simulation

The simulation framework begins with the development of nonlinear structural models capable of representing the response of coastal buildings subjected to both seismic and hydrodynamic loading. As can be seen from Figure 1, structural systems are typically modeled using finite-element formulations that capture the nonlinear behavior of beams, columns, and joints. Rotational spring models are commonly used to represent nonlinear plastic hinge behavior at beam-column connections, while additional springs can capture joint shear failure mechanisms [57,58]. These modeling approaches allow the simulation to represent key damage mechanisms that occur during earthquake excitation, including stiffness degradation, strength deterioration, and plastic rotation accumulation [59]. The structural discretization also enables the representation of hydrodynamic loads acting on seaward columns and structural frames when tsunami waves inundate the building. Such modeling strategies allow the structural model to capture the progressive transition from earthquake-induced damage to tsunami-induced structural failure [57].

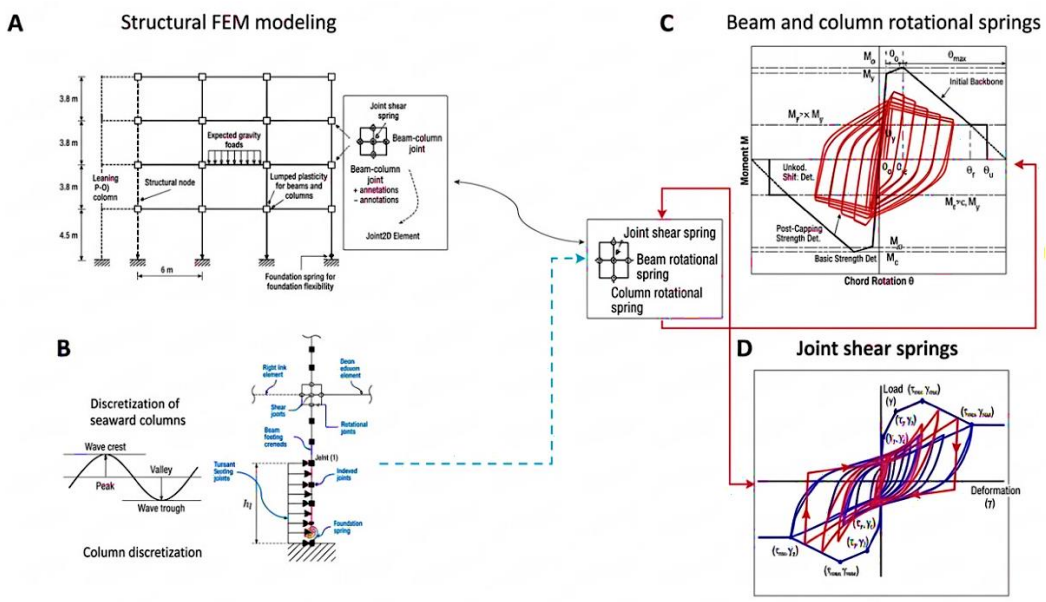

Figure 1. Schematic of the nonlinear FEM model for typical RC frame in US with beam–column rotational springs and joint shear springs used to capture member and joint nonlinear behavior.

Once the structural model is established, the simulation procedure incorporates uncertainties associated with both hazard and structural parameters. As shown in Figure 2, ground motion records representing earthquake excitation are selected from standardized datasets such as the FEMA P-695 (regular-duration earthquakes) and M9 Project (long-duration earthquakes) record sets, which provide a suite of ground motions designed for collapse assessment studies of structural systems (see more details from [58]). These records are scaled to represent a range of seismic intensity levels and applied to the structural model through nonlinear time-history analysis.

 doi:10.20944/preprints202604.1022.v1

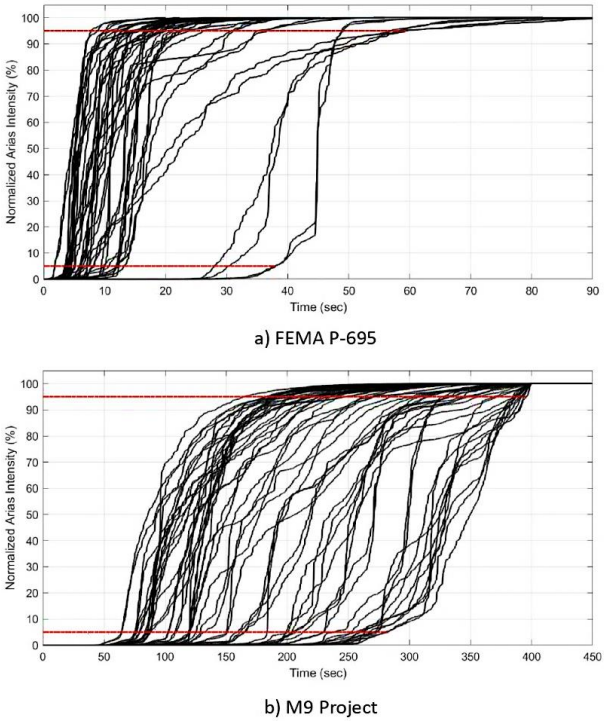

Figure 2. Comparison of regular- and long-duration earthquake records using cumulative energy distribution, motion duration (DS-595) for the earthquake phase of the successive simulation.

The resulting structural response captures the earthquake-induced damage state that forms the initial condition for the subsequent tsunami loading phase. For near-field tsunami scenarios as shown in Figure 3, the structural system may enter the tsunami loading phase with varying levels of residual damage, which significantly influences the structural capacity against hydrodynamic forces [22].

The tsunami loading, in the second phase of the simulation in Figure 3, is represented through hydrodynamic force components acting on the structural frame, typically including drag forces, hydrostatic pressures, and impulsive loads associated with bore impact or velocity contribution of tsunami waves. In the simulation framework, these loads are often represented using simplified hydrodynamic formulations in which the total lateral tsunami force depends on flow depth, flow velocity, and structural geometry. Because tsunami parameters exhibit significant variability, the simulation framework introduces these loads as random variables within a probabilistic modeling framework [57]. Multiple tsunami loading profiles with varying water depths and flow velocities are generated to represent different inundation scenarios (see [57] for more details). This probabilistic treatment allows the simulation to capture the wide range of tsunami forces that may occur during real coastal inundation events.

 doi:10.20944/preprints202604.1022.v1

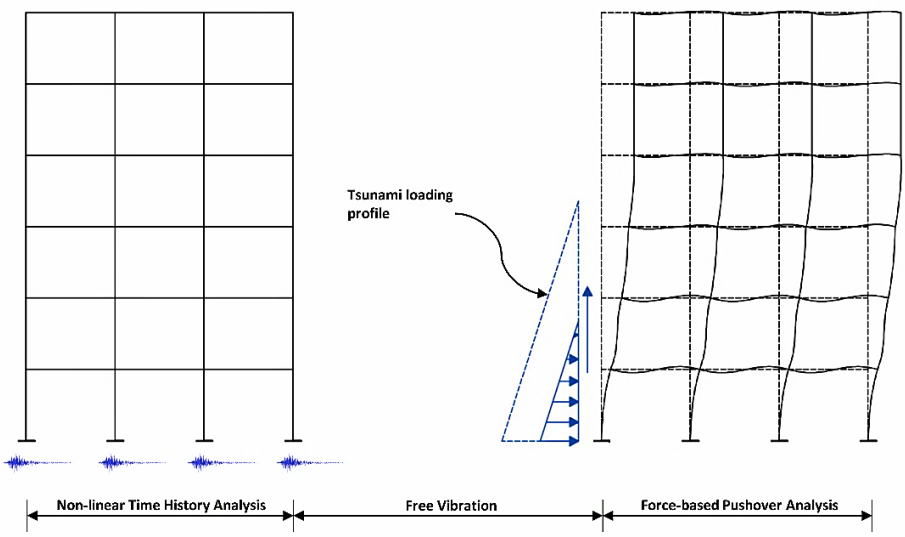

Figure 3. Illustration of the analysis procedure: nonlinear time-history analysis of the structure subjected to earthquake excitation followed by force-based pushover analysis on the deformed structure to evaluate residual capacity.

To evaluate structural performance under combined hazards, the analysis employs a successive hazard simulation strategy as shown earlier in Figure 3. In this process, the earthquake response is first computed through nonlinear dynamic analysis. The damaged structural configuration resulting from the earthquake is then subjected to tsunami loading in a second analysis stage. For each pair of earthquake and tsunami intensity parameters, the structural demand is compared with the structural capacity to determine whether the structure reaches a specified damage state or collapse condition [60]. Repeating this process across a large set of earthquake–tsunami intensity combinations produces a dataset of failure outcomes corresponding to different hazard intensities.

Because the analysis involves multiple sources of uncertainty—including ground motion variability, structural parameter uncertainty, and hydrodynamic load variability—the simulation is typically executed within a Monte Carlo framework. Each realization represents a unique combination of earthquake intensity, tsunami loading conditions, and structural parameters. By performing thousands of such simulations, the analysis produces a large set of outcomes that can be interpreted as realizations of the joint earthquake–tsunami failure process. This computational procedure generates a set of failure probability points that describe the relationship between earthquake intensity measures and tsunami intensity measures for different structural damage states.

3.2. Near-Field Tsunami Fragility Response

The results of the successive simulations using regular-duration earthquakes (FEMA P-695) can be visualized as a set of points representing the conditional failure probability $P(TS \mid EQ)$ across a two-dimensional hazard space. As shown in Figure 4, these points form the basis for constructing fragility surfaces that describe structural vulnerability under combined earthquake–tsunami loading. Surface-fitting techniques can then be applied to the simulated failure probability points in order to obtain continuous fragility surfaces for different damage states [60]. These fragility surfaces provide a generalized representation of structural vulnerability across a wide range of earthquake and tsunami intensities, enabling probabilistic risk assessments that account for interacting hazards [61].

 doi:10.20944/preprints202604.1022.v1

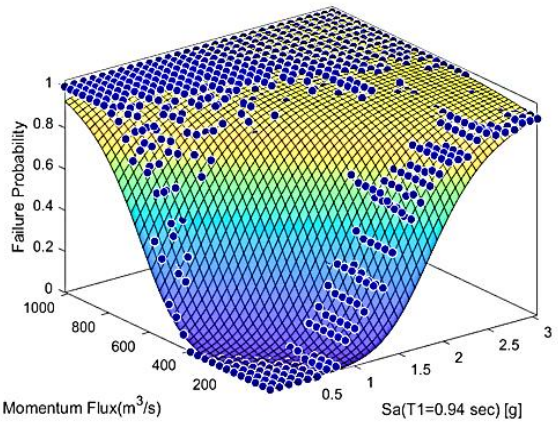

(**a**) Surface fitted to the points of failure probability

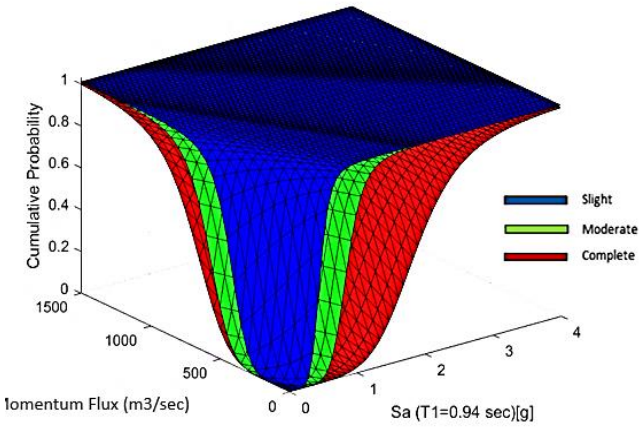

(**b**) Fragility surfaces on different damage states

Figure 4. Multi-hazard fragility surfaces relating spectral acceleration and tsunami momentum flux (MF) to structural damage probability for collapse and multiple damage states.

Validation of the simulation framework is an essential component of the modeling process. For the earthquake component, the nonlinear structural model can be validated by comparing simulated structural responses—such as pushover curves and dynamic fragility curves (Figure 5)—with benchmark results reported in previous studies (e.g., [62,63]). For example, comparisons with established structural models can verify that the simulated building exhibits realistic stiffness, strength, and collapse behavior under seismic loading. Such validation ensures that the earthquake-induced damage states used as initial conditions for tsunami loading are physically consistent and that the component-level modeling assumptions are sound. This step provides confidence that the structural model employed in the second phase of the simulation accurately captures response at the component level, which governs the overall system behavior through its backbone characteristics. It should also be mentioned that the period of vibrations and shape of modes have been also examined and compared to those reported from the benchmarks.

 doi:10.20944/preprints202604.1022.v1

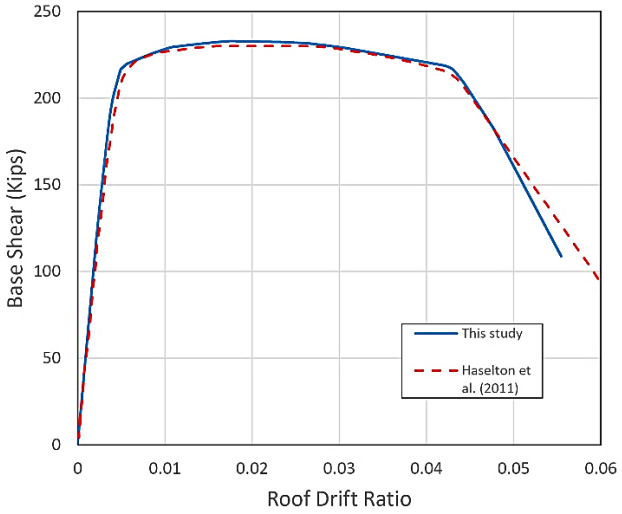

(**a**) Validation on Pushover response

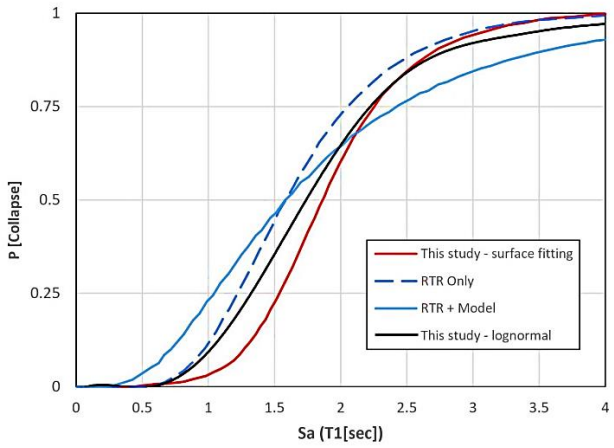

(**b**) Validation of earthquake fragility response

Figure 5. Validation of the structural model. Above: comparison of the pushover response with results reported by Haselton et al. (2011) [62]. Bottom: comparison of the derived earthquake fragility curve with existing models.

For the tsunami component, the resulting fragility curves in Figure 6 can be compared across different earthquake intensity levels to examine how pre-existing earthquake damage influences tsunami vulnerability. In near-field tsunami scenarios, structures subjected to strong earthquake shaking often exhibit an increased baseline probability of failure before tsunami loading begins. As a result, the tsunami fragility curves conditioned on earthquake intensity may exhibit a vertical shift relative to fragility curves derived for undamaged structures. This means that in near-field tsunami fragility simulation, most probability there is a jump at the beginning of the curve where tsunami equivalent force is zero. This jump reflects the compounded damage effect in which the tsunami acts on a structure that has already experienced earthquake-induced degradation. Simulation results, shown in Figure 7, using different earthquake datasets—including those representing long-duration earthquake scenarios (M9 Project earthquakes)—can further illustrate how variations in earthquake characteristics influence the resulting tsunami fragility relationships. And as can be seen in this figure, the jump at the beginning of near-field tsunami fragility curves for long-duration earthquakes are even more pronounced (see [58] for more details).

Preprints.org (www.preprints.org) | NOT PEER-REVIEWED | Posted: 15 April 2026 doi:10.20944/preprints202604.1022.v1

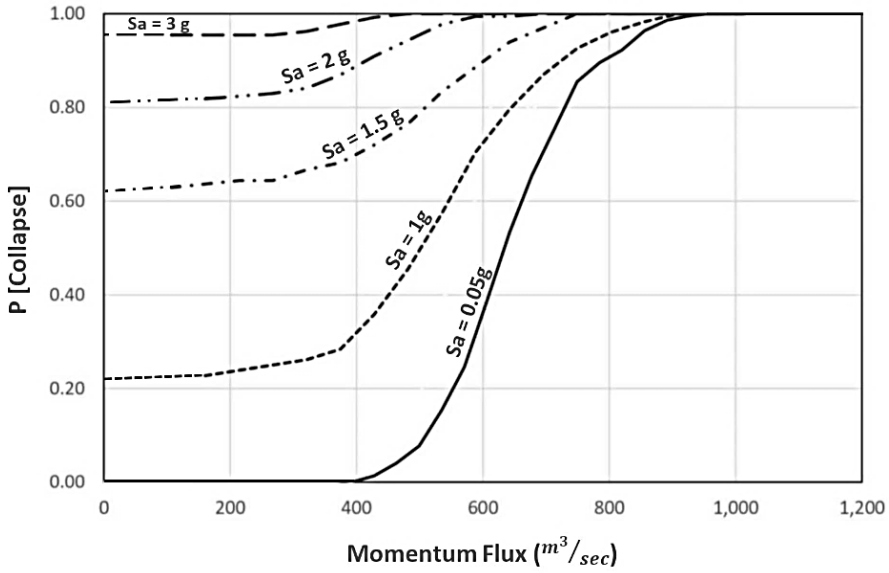

Figure 6. Tsunami fragility curves conditioned on prior earthquake intensity levels, illustrating increased initial failure probability for near-field tsunami scenarios compared to far-field conditions.

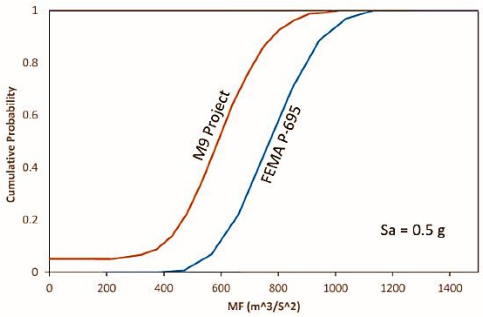

a) Sa = 0.5 g

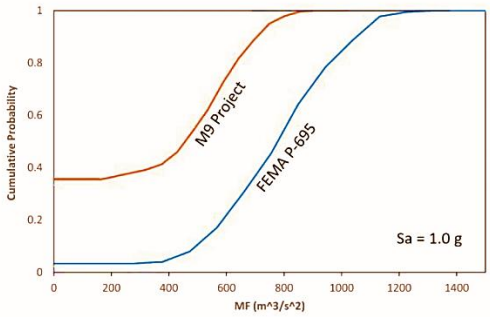

b) Sa = 1.0 g

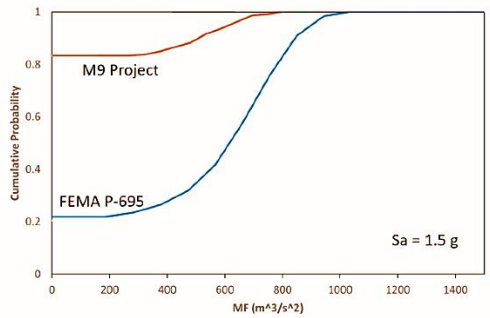

c) Sa = 1.5 g

 doi:10.20944/preprints202604.1022.v1

Figure 7. Comparison of tsunami fragility curves for different earthquake intensity levels (Sa=0.5g, 1.0g, and 1.5g) showing the vertical shift caused by pre-existing earthquake damage prior to tsunami loading.

4. Post-Tsunami Damage Survey

Post-tsunami damage survey datasets provide an essential empirical foundation for understanding how coastal buildings respond to tsunami inundation. While simulation-based fragility modeling enables controlled exploration of structural behavior under coupled earthquake–tsunami hazards, field observations provide direct evidence of real damage mechanisms and allow validation of the simulated fragility relationships [26,64,65]. In this study, post-tsunami survey data are analyzed to examine the relationship between structural damage, hydrodynamic intensity measures, and spatial characteristics such as distance from the coastline. These empirical observations allow the fragility models derived from numerical simulations to be interpreted within the context of actual tsunami damage patterns.

4.1. Damage Survey Data and Information

The damage data utilized in this study are based on the building-level survey dataset compiled by the Japanese Ministry of Land, Infrastructure, Transport and Tourism (MLIT) following the 2011 Great East Japan tsunami [66]. This dataset consists of detailed ex-post damage observations for a large number of structures across multiple affected coastal regions, including Miyako, Rikuzentakata, Minami-Sanriku, Kesennuma, Ishinomaki, Sendai Port, and Sendai Airport [67]. Each record in the dataset includes the observed damage state of individual buildings, categorized into seven discrete levels ranging from no damage (DS1) to washed away (DS7), along with key structural and site-related attributes such as construction type, number of floors, and inundation depth at the building location. The dataset therefore provides a comprehensive empirical basis for linking tsunami intensity measures to structural damage.

In addition to the original survey information, the dataset has been extended in previous studies to incorporate additional geospatial and proxy variables representing hydrodynamic effects, including shielding and debris interaction mechanisms [67]. These extensions also include estimates of tsunami flow velocity, benchmarked against observed inundation patterns across different locations. These enhancements enable a more detailed representation of the complex processes governing tsunami-induced damage while preserving the empirical foundation of the original survey data.

4.2. Observations on Near-Field Tsunamis from Damage Survey

A key insight obtained from the damage survey data is that structural damage exhibits a strong correlation with hydrodynamic intensity measures characterizing tsunami loading. Among these, momentum flux—defined as a function of flow depth and flow velocity—emerges as one of the most informative parameters, as it captures the combined effect of hydrostatic and hydrodynamic forces acting on structures. As illustrated in Figure 8, the probability of failure (exceeding DS4) for wood buildings from damage survey increases nonlinearly with both inundation depth h and flow velocity v, highlighting their coupled influence on damage. The resulting failure surface demonstrates that neither variable alone is sufficient to fully describe structural response; rather, their interaction governs the progression from minor damage to collapse, supporting the use of composite intensity measures such as momentum flux for fragility modeling.

 doi:10.20944/preprints202604.1022.v1

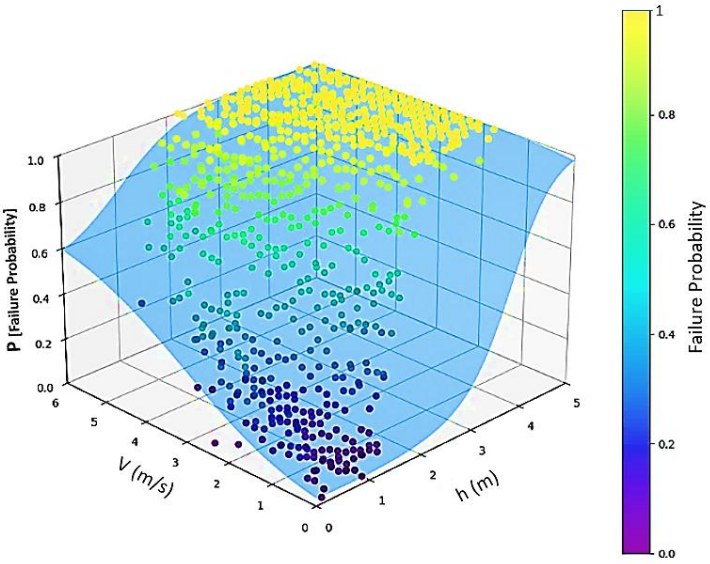

Figure 8. Failure probability surface as a function of inundation depth h and flow velocity v, showing simulation data points and the fitted probabilistic model used to estimate structural failure.

Analysis of the damage survey dataset in Figure 9 shows that the probability of severe structural damage (exceeding DS4) for wood structure type increases systematically with increasing momentum flux values. When the observed damage states are plotted against this hydrodynamic intensity measure, the resulting data points form patterns that resemble the probabilistic fragility relationships obtained from numerical simulations. This observation supports the assumption that hydrodynamic loading parameters such as flow depth, velocity, and their combined momentum flux provide physically meaningful predictors of tsunami-induced structural damage.

Another important observation emerging from the damage survey data is the significant influence of distance from the coastline on observed damage levels. Buildings located closer to the shoreline generally experience higher damage probabilities compared with buildings located further inland. When the dataset is stratified into distance bins measured from the coastline, the resulting fragility curves reveal systematic variations in failure probability with distance. Structures located in the near-coast region tend to exhibit a higher baseline probability of severe damage even at relatively moderate hydrodynamic intensities. In contrast, buildings located farther inland show a lower probability of failure for the same intensity levels. This trend suggests that coastal proximity plays a critical role in tsunami damage processes and should be considered explicitly in fragility modeling frameworks.

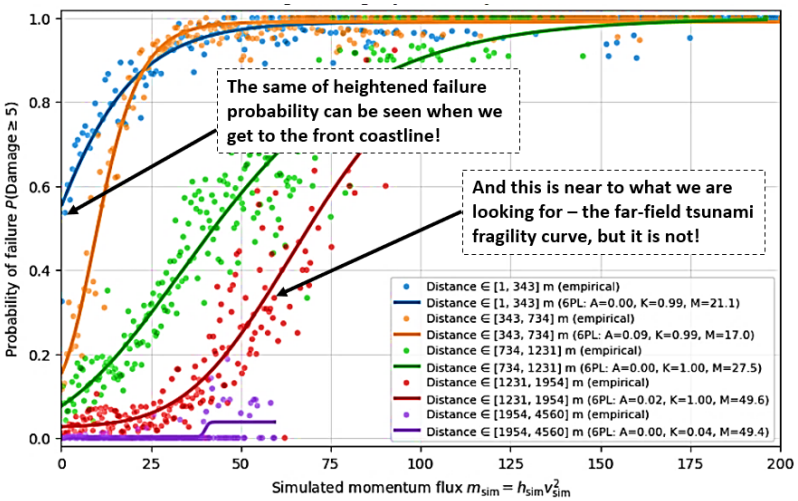

(**a**) Empirical fragility points grouped by distance from coastline

 doi:10.20944/preprints202604.1022.v1

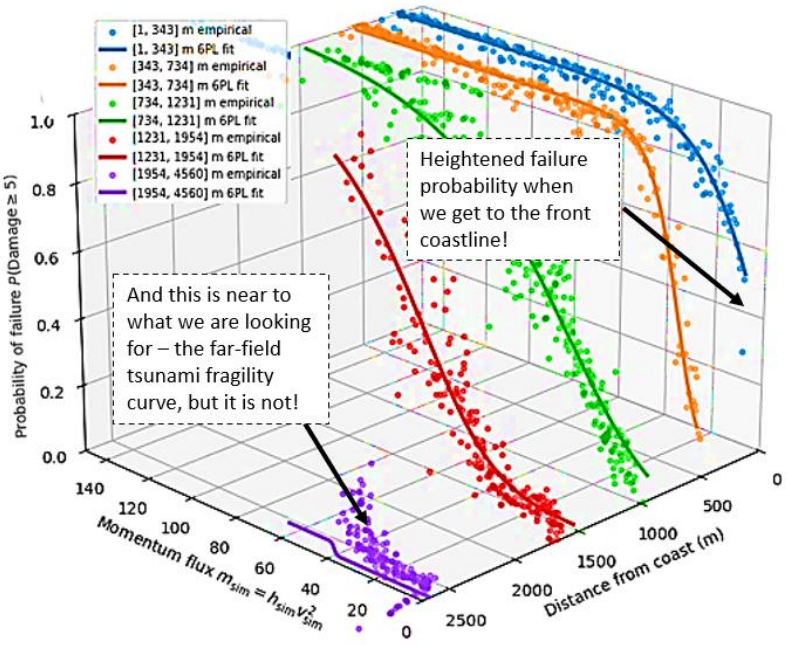

(**b**) 3D fragility for momentum flux versus the distance from coastline

Figure 9. Failure probability surface as a function of simulated momentum flux and distance from the coastline, illustrating the increased initial failure probability near the coast and its influence on tsunami fragility behavior.

The influence of coastal distance on damage patterns also reveals important differences between near-coast, mid-coast, and far-coast tsunami effects. In the immediate coastal zone, buildings are exposed to highly energetic tsunami flows characterized by strong impulsive forces, debris impact, and rapid hydrodynamic loading. These mechanisms contribute to elevated damage probabilities in the near-coast region and can produce structural failures even when hydrodynamic intensity measures appear moderate. In addition, structures in this zone may experience stronger earthquake shaking prior to tsunami arrival, particularly in near-field tsunami events where the earthquake source is located close to the affected coastline. The combined effects of intense tsunami forces and potential earthquake damage lead to elevated fragility levels for buildings located near the shoreline.

At intermediate distances from the coastline, the tsunami flow tends to transition from highly impulsive conditions toward more stable hydrodynamic inundation behavior. In this region, damage patterns are influenced by both the residual energy of the incoming tsunami flow and the attenuation of impulsive forces with distance. As a result, fragility curves derived from damage observations in this region often exhibit intermediate characteristics between near-coast and far-coast behaviors. This transition zone is particularly important for fragility modeling because it captures the gradual attenuation of tsunami forces as the wave propagates inland.

For buildings located further inland, tsunami damage appears to be dominated primarily by hydrodynamic inundation rather than impulsive coastal forces. In these far-coast locations, debris impacts and bore-like forces become less dominant, and the structural response tends to be controlled primarily by sustained hydrodynamic loads. Consequently, the observed damage patterns in this region resemble what is typically described as far-field tsunami fragility behavior, in which structural vulnerability depends mainly on hydrodynamic flow parameters such as water depth and velocity. These conditions align closely with simplified engineering design approaches in which tsunami loads are represented through hydrodynamic pressure formulations, such as those incorporated into design guidance documents and coastal hazard engineering methodologies.

It should be noted that validation of the tsunami edge of the earthquake–tsunami fragility surfaces ideally requires far-field tsunami fragility data, which can serve as a baseline for assessing how numerical simulations perform relative to damage survey observations. However, the tsunami fragility curves presented in Figure 9a,b correspond to near-field conditions. This is because the

 doi:10.20944/preprints202604.1022.v1

survey data were collected in regions where earthquake and tsunami effects were inherently coupled and not distinctly separable. Consequently, none of the curves represent pure far-field tsunami response associated with structures, even for those located relatively distant from the coastline.

Machine-learning-based (ML) analysis—using XGBoost classifier—of the survey dataset further confirms the relative importance of key variables influencing tsunami damage. Feature-importance evaluations presented in Figure 10 show that hydrodynamic parameters such as flow depth and momentum flux are the dominant predictors of structural damage states, followed by distance from the coastline and other environmental variables. This result supports the physical interpretation that tsunami forces are primarily governed by hydrodynamic loading mechanisms, while spatial characteristics influence how those forces are transmitted to the built environment. The classification analysis presented in Figure 10, based on damage states converted to ensure compatibility with IN-CORE metrics [68], demonstrates high predictive accuracy in distinguishing structural damage states. This result indicates that the observed damage patterns exhibit strong statistical relationships with the underlying hazard intensity measures.

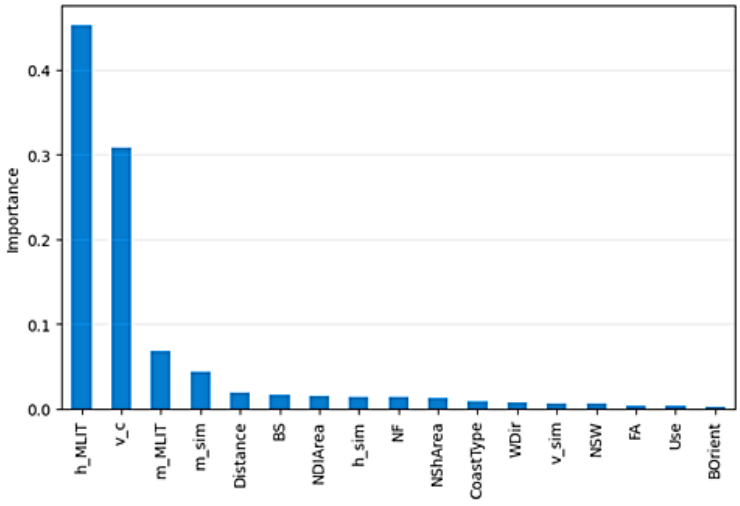

(**a**) Feature Importance Analysis of the variables invoved with the damage survey

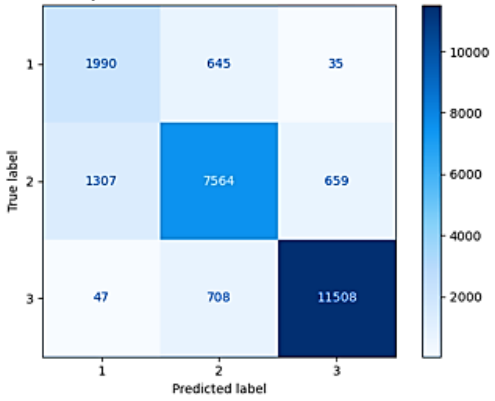

(**b**) Prediction matrix for different damage states

Figure 10. Machine learning model evaluation: feature importance from the XGBoost model for damage prediction (above) and the corresponding confusion matrix showing classification performance across damage states (bottom).

An additional insight from the ML analysis over damage survey data is the identification of coastal attenuation effects in tsunami fragility behavior. As tsunami waves propagate inland, the energy of the flow gradually dissipates due to surface friction, topographic effects, and flow spreading. This attenuation process leads to systematic reductions in tsunami dominant forces with increasing distance from the coastline. When ML-assisted fragility curves derived for different coastal

 doi:10.20944/preprints202604.1022.v1

distance ranges are compared, as shown in Figure 11a, they exhibit systematic shifts toward lower failure probabilities with increasing distance from the coastline. This trend highlights that tsunami fragility relationships are not spatially uniform and must account for the attenuation of hazard intensity across the inundation zone, as illustrated in Figure 11b.

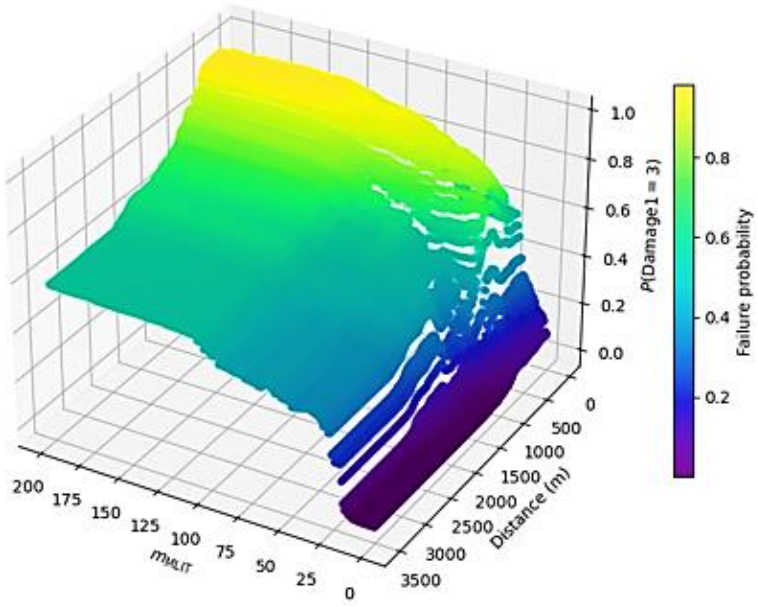

(**a**) Fragility surface of tsunami for momentum flux versus distance from the coastline

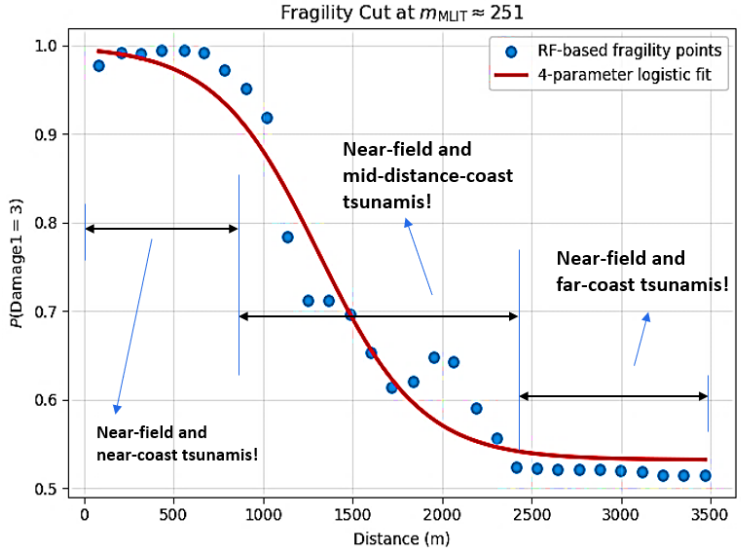

(**b**) Fragility attenuation curve as a function of distance from coastline

Figure 11. Relationship between failure probability and distance from the coastline. Above: probabilistic surface showing failure probability as a function of tsunami intensity and distance from the coast. Bottom: extracted fragility trend illustrating the transition from near-field to far-coast tsunami behavior.

The observed spatial variation in fragility behavior seen from Figure 11b also suggests that fragility curves derived from damage survey data may represent different effective hazard regimes depending on the coastal distance of the surveyed structures. In particular, fragility relationships derived from buildings located far from the shoreline may resemble traditional far-field tsunami fragility curves, while buildings located near the coast may exhibit fragility characteristics influenced by both earthquake damage and intense impulsive tsunami forces. Understanding this distinction is critical when interpreting empirical fragility datasets because the observed damage patterns may reflect a mixture of near-field and far-field tsunami processes.

 doi:10.20944/preprints202604.1022.v1

Figure 12 illustrates the systematic variation of tsunami fragility curves with coastal distance, highlighting the pronounced influence of near-field and near-coast effects on structural vulnerability. As observed, structures located closer to the coastline exhibit significantly higher failure probabilities at lower intensity levels, effectively resulting in a leftward shift of the fragility curve relative to those representing semi–far-field conditions. This behavior suggests that a baseline fragility function developed for far-field tsunami conditions can be adapted to near-field scenarios through an intensity shift that accounts for spatial effects such as amplified hydrodynamic loading, reduced dissipation, and increased debris interaction near the coastline. The proposed shift, expressed as a function of distance, provides a practical mechanism to incorporate near-coast effects without redefining the entire fragility model. Consequently, this approach enables a unified framework in which a reference fragility curve is adjusted based on site-specific characteristics, offering both computational efficiency and physical interpretability in multi-scale tsunami vulnerability assessments.

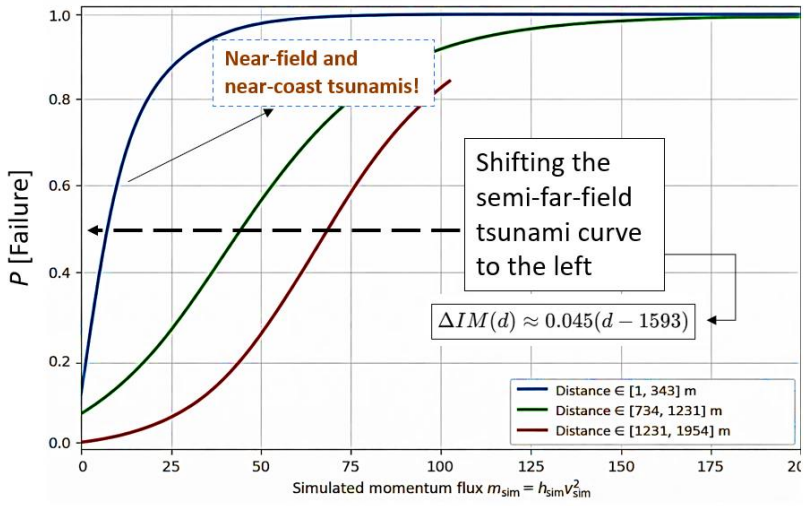

Figure 12. Relationship between failure probability and distance from the coastline. Above: probabilistic surface showing failure probability as a function of tsunami intensity and distance from the coast. Bottom: extracted fragility trend illustrating the transition from near-field to far-coast tsunami behavior.

5. Calibration Challenges for Near-Field Tsunami Fragility

Calibrating fragility relationships for near-field tsunami events remains challenging due to limitations in available empirical data. Although post-event damage surveys exist for major tsunami disasters, they often provide incomplete or inconsistent information on structural damage, hydrodynamic conditions, and spatial characteristics. Key parameters such as flow depth, velocity, and debris effects are rarely measured directly and are instead reconstructed from indirect evidence, introducing significant uncertainty. As a result, existing datasets may not fully capture the range of structural responses under extreme near-field conditions, limiting the robustness of derived fragility relationships.

Uncertainty is further compounded by the complexity of hydrodynamic loading mechanisms and their interaction with structural systems. While common intensity measures such as flow depth, velocity, and momentum flux are used to represent tsunami forces, they do not fully account for impulsive effects such as debris impact, bore pressures, and wave breaking. At the same time, variability in building characteristics—including structural system, material, design quality, and maintenance—leads to significantly different damage outcomes under similar hazard conditions. This heterogeneity makes it difficult to isolate the influence of hazard intensity from structural variability in fragility model calibration.

 doi:10.20944/preprints202604.1022.v1

Another key challenge lies in linking simulation-based results with observed damage states. Numerical models typically express structural response through engineering demand parameters, whereas field surveys classify damage using qualitative or semi-quantitative categories. The lack of standardized mappings between these representations introduces additional uncertainty in both calibration and validation. Moreover, strong spatial heterogeneity in tsunami effects—driven by local topography, coastal geometry, and urban layout—results in significant variations in loading conditions across short distances, further complicating the development of consistent fragility relationships.

Finally, validation of far-field tsunami fragility relationships is limited by the scarcity of suitable empirical data. Most available observations correspond to near-field events, where earthquake and tsunami effects are coupled, whereas many simulation frameworks assume far-field conditions as a baseline. Consequently, validation often relies on laboratory experiments, which introduce additional uncertainties related to scaling and simplifications. Overall, these challenges highlight the need for integrated approaches that combine simulations, field data, and experimental studies to improve the reliability of tsunami fragility modeling.

6. Summary and Conclusions

This study reviewed the development of tsunami fragility relationships by integrating insights from simulation-based structural analysis and post-tsunami damage survey data, with a particular focus on near-field tsunami environments. The results demonstrate that near-field tsunami fragilities cannot be adequately represented using conventional single-hazard or spatially uniform approaches, as structural response is strongly influenced by both preceding earthquake damage and highly variable hydrodynamic loading conditions. The successive simulation framework provides a physically consistent means of capturing these interactions, enabling the direct estimation of conditional fragility relationships without relying on simplified probabilistic assumptions.

Analysis of damage survey data further confirms that tsunami-induced structural damage is governed by coupled hydrodynamic intensity measures, particularly momentum flux, and is significantly influenced by spatial factors such as distance from the coastline. The observed attenuation of fragility with increasing inland distance highlights the importance of accounting for spatial heterogeneity in vulnerability modeling. The proposed interpretation of fragility behavior as a function of coastal distance, including the concept of intensity-based shifting of baseline fragility curves, provides a practical and physically interpretable approach for incorporating near-coast effects into tsunami vulnerability assessments.

At the same time, the study identifies several fundamental challenges in calibrating and validating tsunami fragility models, including limitations in empirical data, uncertainties in hydrodynamic intensity measures, structural variability, and inconsistencies between simulation outputs and observed damage classifications. These challenges are particularly pronounced for near-field tsunami scenarios, where multi-hazard interactions and strong spatial variability complicate both model development and interpretation. The lack of purely far-field empirical datasets further constrains the validation of baseline fragility relationships, emphasizing the need for complementary laboratory and numerical studies.

Acknowledgments: The Center for Risk-Based Community Resilience Planning is a NIST-funded Center of Excellence; the Center is funded through a cooperative agreement between the U.S. National Institute of Standards and Technology and Colorado State University (NIST Financial Assistance Award Numbers: 70NANB15H044 and 70NANB20H008). The views expressed are those of the presenter and may not represent the official position of the National Institute of Standards and Technology or the U.S. Department of Commerce.

 doi:10.20944/preprints202604.1022.v1

References

1. Alam MS, Barbosa AR, Scott MH, Cox DT, van de Lindt JW. Multi-hazard Earthquake-Tsunami Structural Fragility Assessment Framework. Proc. 13th Int. Conf. Appl. Stat. Probab. Civ. Eng. ICASP13, vol. 1, Korean Institute of Bridge and Structural Engineers; 2019, p. 1318–25. https://doi.org/10.22725/ICASP13.244.
2. Amini M, Sanderson DR, Cox DT, Barbosa AR, Rosenheim N. Methodology to incorporate seismic damage and debris to evaluate strategies to reduce life safety risk for multi-hazard earthquake and tsunami. Nat Hazards 2023. https://doi.org/10.1007/s11069-023-05937-8.
3. Charvet I, Suppasri A, Kimura H, Sugawara D, Imamura F. A multivariate generalized linear tsunami fragility model for Kesennuma City based on maximum flow depths, velocities and debris impact, with evaluation of predictive accuracy. Nat Hazards 2015;79:2073–99. https://doi.org/10.1007/s11069-015-1947-8.
4. Foytong P, Ruangrassamee A, Lukkunaprasit P, Thanasisathit N. Behaviours of reinforced-concrete building under tsunami loading. IES J Part Civ Struct Eng 2015;8:101–10. https://doi.org/10.1080/19373260.2015.1013998.
5. Geist EL, Parsons T. Probabilistic Analysis of Tsunami Hazards*. Nat Hazards 2006;37:277–314. https://doi.org/10.1007/s11069-005-4646-z.
6. Probabilistic Tsunami Hazard Analysis: Multiple Sources and Global Applications - Grezio - 2017 - Reviews of Geophysics - Wiley Online Library n.d. https://agupubs.onlinelibrary.wiley.com/doi/full/10.1002/2017RG000579 (accessed March 22, 2026).
7. Cornell CA. Engineering seismic risk analysis. Bull Seismol Soc Am 1968;58:1583–606. https://doi.org/10.1785/BSSA0580051583.
8. Vamvatsikos D, Cornell CA. Incremental dynamic analysis. Earthq Eng Struct Dyn 2002;31:491–514. https://doi.org/10.1002/eqe.141.
9. Ibarra LF, Krawinkler H. Global Collapse of Frame Structures under Seismic Excitations. 2005.
10. Mori N, Goda K, Cox D. Recent Process in Probabilistic Tsunami Hazard Analysis (PTHA) for Mega Thrust Subduction Earthquakes. In: Santiago-Fandiño V, Sato S, Maki N, Iuchi K, editors. 2011 Jpn. Earthq. Tsunami Reconstr. Restor. Insights Assess. 5 Years, Cham: Springer International Publishing; 2018, p. 469–85. https://doi.org/10.1007/978-3-319-58691-5_27.
11. Behrens J, Løvholt F, Jalayer F, Lorito S, Salgado-Gálvez MA, Sørensen M, et al. Probabilistic Tsunami Hazard and Risk Analysis: A Review of Research Gaps. Front Earth Sci 2021;9:628772. https://doi.org/10.3389/feart.2021.628772.
12. Reis C, Baptista MA, Lopes M, Oliveira CS, Clain S. Cascade earthquake and tsunami hazard assessment: A deterministic perspective for engineering purposes. Int J Disaster Risk Reduct 2022;75:102952. https://doi.org/10.1016/j.ijdrr.2022.102952.
13. Ma T, Shen L, Chen Z, Liang D. Review on tsunami research and risk mitigation: from prediction models to resilient coastal communities. Npj Nat Hazards 2026;3:34. https://doi.org/10.1038/s44304-026-00195-7.
14. Zamora N, Grezio A, Papathoma-Köhle M, Jalayer F, Salmanidou D, Parsons T, et al. Frameworks for Assessing Tsunami Hazard and Risk. In: Sørensen MB, Behrens J, Jalayer F, Løvholt F, Lorito S, Rafliana I, et al., editors. Probabilistic Tsunami Hazard Risk Anal. Cookb., Cham: Springer Nature Switzerland; 2026, p. 13–86. https://doi.org/10.1007/978-3-031-98115-9_2.
15. Gibbons SJ, Lorito S, Macías J, Løvholt F, Selva J, Volpe M, et al. Probabilistic Tsunami Hazard Analysis: High Performance Computing for Massive Scale Inundation Simulations. Front Earth Sci 2020;8. https://doi.org/10.3389/feart.2020.591549.
16. Gunawan WC, Alhamid AK, Akiyama M, Permana MF, Farid M, Kurniawan A, et al. Probabilistic tsunami risk assessment based on supervised learning considering nonstationary sea-level rise and multiple source rupture: Application to Denpasar City of Bali. Prog Disaster Sci 2026;29:100505. https://doi.org/10.1016/j.pdisas.2025.100505.
17. De Risi R, Goda K. Probabilistic Earthquake-tsunami Hazard Assessment: The First Step Towards Resilient Coastal Communities. Procedia Eng 2017;198:1058–69. https://doi.org/10.1016/j.proeng.2017.07.150.
18. Renn O. New challenges for risk analysis: systemic risks. J Risk Res 2021;24:127–33.

 doi:10.20944/preprints202604.1022.v1

19. Rafliana I, Jalayer F, Cerase A, Cugliari L, Baiguera M, Salmanidou D, et al. Tsunami risk communication and management: Contemporary gaps and challenges. Int J Disaster Risk Reduct 2022;70:102771. https://doi.org/10.1016/j.ijdrr.2021.102771.
20. Jalayer F, Ebrahimian H, Trevlopoulos K, Bradley B. Empirical tsunami fragility modelling for hierarchical damage levels. Nat Hazards Earth Syst Sci 2023;23:909–31. https://doi.org/10.5194/nhess-23-909-2023.
21. Charvet I, Macabuag J, Rossetto T. Estimating Tsunami-Induced Building Damage through Fragility Functions: Critical Review and Research Needs. Front Built Environ 2017;3. https://doi.org/10.3389/fbuil.2017.00036.
22. Attary N, Van De Lindt JW, Barbosa AR, Cox DT, Unnikrishnan VU. Performance-Based Tsunami Engineering for Risk Assessment of Structures Subjected to Multi-Hazards: Tsunami following Earthquake. J Earthq Eng 2021;25:2065–84. https://doi.org/10.1080/13632469.2019.1616335.
23. O'BRIEN K, ERIKSEN S, NYGAARD LP, SCHJOLDEN A. Why different interpretations of vulnerability matter in climate change discourses. Clim Policy 2007;7:73–88. https://doi.org/10.1080/14693062.2007.9685639.
24. Xiong Y, Liang Q, Park H, Cox D, Wang G. A deterministic approach for assessing tsunami-induced building damage through quantification of hydrodynamic forces. Coast Eng 2019;144:1–14. https://doi.org/10.1016/j.coastaleng.2018.11.002.
25. Rodwell J, Williams JH, Paulik R. Empirical Fragility Assessment of Three-Waters and Railway Infrastructure Damaged by the 2015 Illapel Tsunami, Chile. J Mar Sci Eng 2023;11:1991. https://doi.org/10.3390/jmse11101991.
26. Oddo MC, Cavaleri L. Earthquake-tsunami combined fragility curves for coastal masonry buildings: a numerical-analytical approach. Bull Earthq Eng 2025. https://doi.org/10.1007/s10518-025-02147-4.
27. Sannikova NK, Segur H, Arcas D. Influence of Tsunami Aspect Ratio on Near and Far-Field Tsunami Amplitude. Geosciences 2021;11:178. https://doi.org/10.3390/geosciences11040178.
28. Sharrocks PD, Peakall J, Hodgson DM, Barlow NLM. Tsunami versus storms: Diagnostic sedimentary criteria in coastal lakes, lagoons and sinkhole deposits. Earth-Sci Rev 2025;271:105277. https://doi.org/10.1016/j.earscirev.2025.105277.
29. Laksono FAT, Mishra M, Fadlin, Kovács J. Exploring the tsunami generation potential of major faults in the sicilian channel using 3D numerical modeling. Ocean Model 2026;199:102625. https://doi.org/10.1016/j.ocemod.2025.102625.
30. Tappin DR. The Generation of Tsunamis. Encycl. Marit. Offshore Eng., John Wiley & Sons, Ltd.; 2017, p. 1–10. https://doi.org/10.1002/9781118476406.emoe523.
31. Vilibić I, Zemunik Selak P, Šepić J. Meteorological Tsunamis: From Local Hazard to Global Relevance. Rev Geophys 2025;63:e2024RG000867. https://doi.org/10.1029/2024RG000867.
32. Schindelé F, Kong L, Lane EM, Paris R, Ripepe M, Titov V, et al. A Review of Tsunamis Generated by Volcanoes (TGV) Source Mechanism, Modelling, Monitoring and Warning Systems. Pure Appl Geophys 2024;181:1745–92. https://doi.org/10.1007/s00024-024-03515-y.
33. Abdelhafeez M, Park H, Sherif M, Ghanem A, Moon D-S. Effects of tsunami wave and bathymetric parameters on hydrodynamic forces and structural fragility. J Build Eng 2026;118:115077. https://doi.org/10.1016/j.jobe.2025.115077.
34. Kolukula SS, Murty PLN, Kumar TS, Ramarao EP, M. V RM. Tsunami modelling over global oceans. R Soc Open Sci 2025;12:241128. https://doi.org/10.1098/rsos.241128.
35. Tsunami Hazard Assessment Based on Wave Generation, Propagation, and Inundation Modeling for the U.S. East Coast (NUREG/CR-7222) | Nuclear Regulatory Commission n.d. https://www.nrc.gov/reading-rm/doc-collections/nuregs/contract/cr7222/index (accessed March 22, 2026).
36. Koshimura S, Oie T, Yanagisawa H, Imamura F. Developing Fragility Functions for Tsunami Damage Estimation Using Numerical Model and Post-Tsunami Data from Banda Aceh, Indonesia. Coast Eng J 2009;51:243–73. https://doi.org/10.1142/S0578563409002004.
37. Sturm M, Gems B, Keller F, Mazzorana B, Fuchs S, Papathoma-Köhle M, et al. Experimental analyses of impact forces on buildings exposed to fluvial hazards. J Hydrol 2018;565:1–13. https://doi.org/10.1016/j.jhydrol.2018.07.070.

 doi:10.20944/preprints202604.1022.v1

38. Koh MJ, Park H, Kim AS. Tsunami-driven debris hazard assessment at a coastal community: Focusing on shipping container debris hazards at Honolulu Harbor, Hawaii. Coast Eng 2024;187:104408. https://doi.org/10.1016/j.coastaleng.2023.104408.
39. Nistor I, Goseberg N, Stolle J. Tsunami-Driven Debris Motion and Loads: A Critical Review. Front Built Environ 2017;3. https://doi.org/10.3389/fbuil.2017.00002.
40. De Risi R, Goda K, Yasuda T, Mori N. Is flow velocity important in tsunami empirical fragility modeling? Earth-Sci Rev 2017;166:64–82. https://doi.org/10.1016/j.earscirev.2016.12.015.
41. Park H, Cox DT. Probabilistic assessment of near-field tsunami hazards: Inundation depth, velocity, momentum flux, arrival time, and duration applied to Seaside, Oregon. Coast Eng 2016;117:79–96. https://doi.org/10.1016/j.coastaleng.2016.07.011.
42. Del Zoppo M, Di Ludovico M, Lignola GP, Prota A. Time-dependent tsunami fragility analysis for reinforced concrete building stock. Eng Struct 2025;330:119931. https://doi.org/10.1016/j.engstruct.2025.119931.
43. Harati M, van de Lindt JW. Data-driven machine learning for multi-hazard fragility surfaces in seismic resilience analysis. Comput-Aided Civ Infrastruct Eng 2024:mice.13356. https://doi.org/10.1111/mice.13356.
44. Reis C, Lopes M, Baptista MA, Clain S. Towards an integrated framework for the risk assessment of coastal structures exposed to earthquake and tsunami hazards. Resilient Cities Struct 2022;1:57–75. https://doi.org/10.1016/j.rcns.2022.07.001.
45. Considering the Potential Impact of Tsunamis on Structures n.d. https://www.structuremag.org/article/considering-the-potential-impact-of-tsunamis-on-structures/ (accessed March 22, 2026).
46. Rea R, Scala A, Bernardi F, Elia L, Lorito S, Colombelli S, et al. Feasibility study of an integrated earthquake and tsunami early warning system. Sci Rep 2025;15:43124. https://doi.org/10.1038/s41598-025-25832-5.
47. Belliazzi S, Lignola GP, Palermo D. Simplified structural analysis framework for buildings under combined earthquake and tsunami loads. Structures 2025;77:109206. https://doi.org/10.1016/j.istruc.2025.109206.
48. Macabuag J, Rossetto T, Ioannou I, Eames I. Investigation of the Effect of Debris-Induced Damage for Constructing Tsunami Fragility Curves for Buildings. Geosciences 2018;8:117. https://doi.org/10.3390/geosciences8040117.
49. Park S, van de Lindt JW, Cox D, Gupta R, Aguiniga F. Successive Earthquake-Tsunami Analysis to Develop Collapse Fragilities. J Earthq Eng 2012;16:851–63. https://doi.org/10.1080/13632469.2012.685209.
50. Goda K, Catalan PA. Risk-based multi-hazard microzonation for earthquakes and tsunamis. Front Earth Sci 2025;13. https://doi.org/10.3389/feart.2025.1568069.
51. Grezio A, Babeyko A, Baptista MA, Behrens J, Costa A, Davies G, et al. Probabilistic Tsunami Hazard Analysis: Multiple Sources and Global Applications. Rev Geophys 2017;55:1158–98. https://doi.org/10.1002/2017RG000579.
52. Alam MS, Barbosa AR, Scott MH, Cox DT, van de Lindt JW. Development of Physics-Based Tsunami Fragility Functions Considering Structural Member Failures. J Struct Eng 2018;144:04017221. https://doi.org/10.1061/(ASCE)ST.1943-541X.0001953.
53. Alam MS, Winter AO, Galant G, Shekhar K, Barbosa AR, Motley MR, et al. Tsunami-Like Wave-Induced Lateral and Uplift Pressures and Forces on an Elevated Coastal Structure. J Waterw Port Coast Ocean Eng 2020;146:04020008. https://doi.org/10.1061/(ASCE)WW.1943-5460.0000562.
54. Attary N, Unnikrishnan VU, van de Lindt JW, Cox DT, Barbosa AR. Performance-Based Tsunami Engineering methodology for risk assessment of structures. Eng Struct 2017;141:676–86. https://doi.org/10.1016/j.engstruct.2017.03.071.
55. Harati M, van de Lindt JW. Physics-based earthquake-tsunami fragility surfaces for risk and resilience analysis. 2024. https://doi.org/10.1201/9781003483755-390.
56. FEMA P-646 Guidelines for Design of Structures for Vertical Evacuation from Tsunamis, 3rd Edition | WBDG - Whole Building Design Guide 2019. https://www.wbdg.org/ffc/dhs/criteria/femap646 (accessed November 30, 2022).
57. Harati M, van de Lindt JW. Methodology to generate earthquake-tsunami fragility surfaces for community resilience modeling. Eng Struct 2024;305:117700. https://doi.org/10.1016/j.engstruct.2024.117700.

 doi:10.20944/preprints202604.1022.v1

58. Harati, van de Lindt. Impact of Long-duration Earthquakes on Successive Earthquake-tsunami Fragilities for Reinforced Concrete Frame Archetypes. J Struct Eng 2024;150:1–19.
59. Harati M, van de Lindt JW. Mainshock-aftershock building fragility methodology for community resilience modeling. Structures 2024;70:107742. https://doi.org/10.1016/j.istruc.2024.107742.
60. Harati, Mojtaba, van de Lindt, John W. Fragility Function Development of RC Building Portfolio for Use in Earthquake-Tsunami Community Resilience Studies. J Perform Constr Facil 2024.
61. Harati, Mojtaba, van de Lindt, John W. Community-Level Resilience Analysis using Earthquake-Tsunami Fragility Surfaces. Resilient Cities Struct 2024.
62. Haselton CB, Liel AB, Deierlein GG, Dean BS, Chou JH. Seismic Collapse Safety of Reinforced Concrete Buildings. I: Assessment of Ductile Moment Frames. J Struct Eng 2011;137:481–91. https://doi.org/10.1061/(ASCE)ST.1943-541X.0000318.
63. Liel AB, Haselton CB, Deierlein GG. Seismic Collapse Safety of Reinforced Concrete Buildings. II: Comparative Assessment of Nonductile and Ductile Moment Frames. J Struct Eng 2011;137:492–502. https://doi.org/10.1061/(ASCE)ST.1943-541X.0000275.
64. Dias WPS, Yapa HD, Peiris LMN. Tsunami vulnerability functions from field surveys and Monte Carlo simulation. Civ Eng Environ Syst 2009;26:181–94. https://doi.org/10.1080/10286600802435918.
65. Suppasri A, Mas E, Charvet I, Gunasekera R, Imai K, Fukutani Y, et al. Building damage characteristics based on surveyed data and fragility curves of the 2011 Great East Japan tsunami. Nat Hazards 2013;66:319–41. https://doi.org/10.1007/s11069-012-0487-8.
66. Scorzini AR, Di Bacco M, Sugawara D, Suppasri A. Extended MLIT dataset for the 2011 Great East Japan tsunami with inclusion of velocity information 2024;1. https://doi.org/10.17632/5m3n2hjwkh.1.
67. Scorzini AR, Di Bacco M, Sugawara D, Suppasri A. Machine learning and hydrodynamic proxies for enhanced rapid tsunami vulnerability assessment. Commun Earth Environ 2024;5:301. https://doi.org/10.1038/s43247-024-01468-7.
68. van de Lindt JW, Kruse J, Cox DT, Gardoni P, Lee JS, Padgett J, et al. The interdependent networked community resilience modeling environment (IN-CORE). Resilient Cities Struct 2023;2:57–66. https://doi.org/10.1016/j.rcns.2023.07.004.